Regulation of sugar metabolism genes in the N-dependent susceptibility of tomato stems to Botrytis cinerea

Nathalie Lacrampe, Félicie Lopez-Lauri, Raphaël Lugan, Sophie Colombié, Jérôme Olivares, Philippe C. Nicot, François Lecompte

HAL Id: hal-02954833
https://hal.inrae.fr/hal-02954833v1

Regulation of sugar metabolism genes in the N-dependent susceptibility of tomato stems to *Botrytis cinerea*

Nathalie LACRAMPE[1,2], Félicie LOPEZ-LAURI[2], Raphaël LUGAN[2], Sophie COLOMBIÉ[3], Jérôme OLIVARES[1], Philippe C. NICOT[4] and François LECOMPTE[1,*]

[1] *PSH unit, INRAE, F-84914 Avignon, France ;* [2] *UMR Qualisud, Avignon Université, F-84916 Avignon, France ;* [3] *UMR 1332 BFP, INRAE, Univ Bordeaux, F-33883 Villenave d'Ornon, France ;* [4] *Plant pathology unit, INRAE, F-84140 Montfavet, France*

* *For correspondence. E-mail francois.lecompte.2@inrae.fr*

- **Background and Aims** The main soluble sugars are important components of plant defence against pathogens, but the underlying mechanisms are unclear. Upon infection by *Botrytis cinerea*, the activation of several sugar transporters, from both plant and fungus, illustrates the struggle for carbon resources. In sink tissues, the metabolic use of the sugars mobilized in the synthesis of defence compounds or antifungal barriers is not fully understood.

- **Methods** In this study, the nitrogen-dependent variation of tomato stem susceptibility to *B. cinerea* was used to examine – before and throughout the course of infection – the transcriptional activity of enzymes involved in sugar metabolism. Under different nitrate nutrition regimes, the expressions of genes that encode the enzymes of sugar metabolism (invertases, sucrose synthases, hexokinases, fructokinases and phosphofructokinases), as well as sugar contents, were measured before inoculation and in asymptomatic tissues surrounding the lesions after inoculation.

- **Key Results** At high nitrogen availability, decreased susceptibility was associated with the over-expression of several genes two days after inoculation: sucrose synthase *Sl-SUS1* and *Sl-SUS3*, cell wall invertase *Sl-LIN5* to *Sl-LIN9* and some fructokinase and phosphofructokinase genes. By contrast, increased susceptibility corresponded to the early repression of several genes that encode cell wall invertase and sucrose synthase. The evolution of sugar contents was coherent with the gene expressions.

2

- **Conclusions** The activation of specific genes which encode sucrose synthase is required for enhanced defence. Since the over-expression of fructokinase is also associated with reduced susceptibility, it can be hypothesized that supplemental sucrose cleavage by sucrose synthases is dedicated to the production of cell wall components from UDP-glucose, or to the additional implication of fructose for the synthesis of antimicrobial compounds, or both.

Key words: *Botrytis cinerea*, fructokinase, hexokinase, invertase, nitrate, plant pathogen interaction, *Solanum lycopersicum* (Tomato), sucrose synthase.

INTRODUCTION

The leaves of healthy plants synthetize carbohydrates through photosynthesis and they export sucrose, which is carried via the phloem, and unloaded in sink tissues such as stems, roots or fruit, via sucrose transporters (SWEET transporters) or plasmodesmata (Ruan, 2014). Once inside the parenchyma of sink tissues, the sucrose can enter the cells via transporters, or be cleaved in the apoplast by cell wall invertases (EC 3.2.1.26) into glucose and fructose, which are then imported into the cytoplasm via hexose transporters (Sugar Transporters Proteins). Cytosolic sucrose can be stored in vacuoles and eventually cleaved into glucose and fructose by a vacuolar invertase. Cytosolic sucrose can also be reversibly cleaved by sucrose synthases (EC 2.4.1.13), thus yielding fructose and UDP-glucose, the latter being a precursor of cell wall polysaccharides (Proels and Hückelhoven, 2014; Stein and Granot, 2019). Glucose and fructose enter the glycolysis after phosphorylation by hexokinases (EC 2.7.1.1) or fructokinases (EC 2.7.1.4). Hexokinases are the only known enzymes able to phosphorylate glucose, but they can also phosphorylate fructose, however with lower affinity (Pego and Smeekens, 2000; Granot, 2007; Paulina Aguilera-Alvarado and Sanchez-Nieto, 2017; Stein and Granot, 2018). In the next step of glycolysis, glucose-6-phosphate is converted into fructose-6-phosphate, which is phosphorylated by phosphofructokinases (EC 2.7.1.11) into fructose-1,6-bisphosphate.

Most of the genes that encode these enzymes have already been described in tomato. *Sl-LIN5* to *Sl-LIN9* encode for cell wall invertases, *Sl-VI* for a vacuolar invertase and *Sl-NI* for a mitochondrial invertase. *Sl-SUS1* and *Sl-SUS3* to *Sl-SUS7* encode for six sucrose synthase isozymes. Among the hexokinase genes *Sl-HXK1* to *Sl-HXK6*, three are located in the cytosol, and associated with the mitochondrial membrane (*Sl-HXK1* to *Sl-HXK3*), one is plastidial (*Sl-HXK4*) and two have not been located (*Sl-HXK5* and *Sl-HXK6*). Among the four fructokinases reported in the literature, three are cytosolic (*Sl-FRK1*, *Sl-FRK2* and *Sl-FRK4*)

4

and one is plastidial (*Sl-FRK3*). In addition, eight putative phosphofructokinases have been identified in the tomato genome (*Sl-PFK1* to *Sl-PFK8*).

Host sugars play a central role in plant-pathogen interactions (Rojas *et al.*, 2014). The main soluble sugars such as sucrose, glucose and fructose are thought to be involved both in the production and the regulation of anti-fungal metabolites, the maintenance of cell homeostasis, and they can also be used as a substrate for pathogen growth (Morkunas and Ratajczak, 2014). During pathogen infection, the host metabolism is substantially altered. The pathogen colonization of plant source tissues induces an inhibition of photosynthesis along with an activation of respiratory processes such as glycolysis, the TCA cycle, and the mitochondrial electron transport chain, which are required for defence (Berger *et al.*, 2007; Kanwar and Jha, 2019). The host cell machinery is manipulated by many pathogens for nutrient release (Fatima and Senthil-Kumar, 2015; Oliva and Quibod, 2017). Biotic stresses have been found to increase cell wall invertase activity (Berger *et al.*, 2007; Bolton, 2009; Proels and Hückelhoven, 2014) and to alter sucrose synthase at different levels: the gene expression in leaf veins and syncytia (Hren *et al.*, 2009; Cabello *et al.*, 2014), the protein level in the phloem (Brzin *et al.*, 2011), and the enzymatic activity in the wheat spikelet (Rios *et al.*, 2017).

Botrytis cinerea is a plant pathogenic fungus with a broad host range. Unlike biotrophs, necrotrophic pathogens such as *B. cinerea* kill host cells and feed on decayed tissues (Glazebrook, 2005). The metabolic adaptation of the host to infection by necrotrophic fungi has not fully been elucidated. An inhibition of photosynthesis activity measured using chlorophyll fluorescence was observed in tomato leaves infected by *B. cinerea* (Berger *et al.*, 2004). Gene transcripts linked to photosynthesis activity were also repressed in *Arabidopsis* leaves (Windram *et al.*, 2012), lettuce leaves (De Cremer *et al.*, 2013) and immature grape berries (Agudelo-Romero *et al.*, 2015). However, an increased photosynthetic rate was also

5

observed in the area surrounding the infection site of tomato leaves (Berger *et al.*, 2004). In addition, sugar transport may undergo severe modification during *Botrytis* infection. In *Arabidopsis*, the pathogen was shown to highjack host sugar efflux systems by the direct induction of genes that encode SWEET transporters such as *At-SWEET4*, *At-SWEET7* and *At-SWEET15*, thus promoting pathogenesis (Chen *et al.*, 2010; Oliva and Quibod, 2017). However, genes that encode *At-STP4* and *At-STP13* Sugar Transporter Proteins, causing sugar influx, may also be induced and play a role in plant defence (Fotopoulos *et al.*, 2003; Lemonnier *et al.*, 2014). The struggle for available sugars may involve the induction of cell wall invertases as well. Although the activity of invertase can be controlled at the post-translational level via their reaction products or inhibitory proteins (Fotopoulos, 2005), a higher transcriptional activity of invertase genes was reported after a *Botrytis* infection. This was the case, for example, for *Sl-LIN6* in tomato (Berger *et al.*, 2004) and *At-βfruct1* in *Arabidopsis* (Fotopoulos *et al.*, 2003). Moreover, hexokinases are known to play a major role in defence, presumably as glucose sensors and regulators of gene expressions (Rojas *et al.*, 2014; Aguilera-Alvarado and Sanchez-Nieto, 2017). The over-expression of two *At-HXK* genes in *Arabidopsis* increased the resistance to necrotrophic fungi (Sarowar *et al.*, 2008).

The inhibition of photosynthetic mechanisms, along with the modulation of the enzymes implicated in carbohydrate metabolism, may lead to a modification of sugar contents in infected tissues. In *Botrytis*-infected tomato leaves, sugar levels decreased with an increase in the hexose-to-sucrose ratio (Berger *et al.*, 2004, 2007; Camañes *et al.*, 2015). However, in grape berries, the establishment of a pathogen-induced sink was reported, with an observed increase in fructose and glucose contents (Agudelo-Romero *et al.*, 2015). The balance between host and pathogen sugar utilization may define the outcome of the interaction. The manipulation of constitutive sugar equilibria through variations of host nitrogen nutrition in lettuce (Lecompte *et al.*, 2013) and tomato (Lecompte *et al.*, 2017)

6

showed that the relative concentrations of sucrose and hexose to the total sugar content were good markers of the plant's susceptibility to *B. cinerea* and lesion growth a few days after inoculation. Moreover, the differentiated evolution of glucose and fructose contents in tomato stems after infection suggested that fructose played a specific role in the defence process.

In the present work, we used the nitrogen-dependent variation of tomato stem susceptibility to *B. cinerea* to examine the transcriptional activity of selected enzymes: invertases, sucrose synthases, hexokinases, fructokinases and phosphofructokinases before and throughout the course of infection.

MATERIALS AND METHODS

Plant production and nitrate treatments

Protocols similar to those previously described (Lecompte *et al.*, 2010, 2017) were used in this experiment. Plants were grown in a glasshouse from February to March 2018. Tomato seeds (*Solanum lycopersicum* cultivar "Clodano", Syngenta, Wilmington, DE, USA) were sown and the seedlings were transferred, ten days after germination, onto $7 \times 7 \times 6$ cm rock wool blocks. After three additional weeks, the plants (bearing 3-4 leaves) were placed on top of 2 L pots filled with a mixture (1:1 v/v) of vermiculite and pozzolana. From the germination to the beginning of the N-treatment, the plants were fertigated twice a day with a standard commercial nutrient solution (Liquoplant rose, Plantin, Courthézon, France). N-treatments were started seven weeks after germination. Four nutrient solutions were used, containing nitrate concentrations of 0.5, 2, 10 and 20 mM. It had been previously shown in similar experiments that 10 mM is the optimal concentration for growth, and that 20 mM corresponded to an excess of nitrogen supply, while 0.5 and 2 mM corresponded to severe and mild nitrogen stresses, respectively. In the solutions with lower nitrate concentrations, the equilibrium in electric charges was maintained by replacing nitrates (monovalent anions)

7

with sulphates (divalent anions), up to 7.5 mM SO_4^{2-} in the solution containing the lowest nitrate concentration, 0.5 mM NO_3^-. This substitution is unlikely to have affected plant growth since tomato is known not to be affected by very high sulphate supply concentrations (Lopez *et al*, 1996). The concentration of other major nutrient elements was kept constant, at the following levels: 10 mM K^+, 3.5 mM Mg^{2+}, 3.25 mM Ca^{2+} and 0.02 mM HPO_4^{2-}. Micronutrients were present at the following concentrations (in µM): 0.5 B, 0.02 Cu^{2+}, 8.2 Fe^{2+}, 0.5 Mn^{2+}, 0.01 MoO_4^{2-} and 0.1 Zn^{2+}. The plants were fertigated using a drip irrigation system (one dripper per pot) up to nine times a day depending on the climatic demand, with two-minute pulses. All plants received the same amount of water. The pH was adjusted to 6.0 in each treatment by adding H_3PO_4.

Inoculation of leaf pruning wounds with conidia of B. cinerea

Botrytis cinerea strain BC1 was grown on plates containing potato dextrose agar medium (PDA; Difco, Detroit, MI, USA) in a growth chamber (18°C night, 22°C day, and 14-h daylight). Conidia were collected in sterile ultra-pure water from the surface of 14-day-old cultures. Each suspension was filtered through a 30 µm mesh sterile filter to remove mycelium fragments, and adjusted to a concentration of 10^7 conidia mL^{-1} with the help of a haemocytometer.

Thirty-five plants were used for each N-treatment, corresponding to seven batches of five biological replicates, sampled just before inoculation (0 days post inoculation, DPI), and at 2, 4 and 7 DPI (one batch of mock-inoculated and one batch of *Botrytis*-inoculated plants at each date). Inoculations were carried out in the morning (between 0900h and 1000h, local time) on the petiole stubs (5-7 mm long) that remained on the stems after the excision of the sixth leaf. The wounds received a 10 µL aliquot of either the spore suspension (*Botrytis*-inoculated plants) or sterile water (mock-inoculated plants).

To foster disease development, the *Botrytis*- and mock-inoculated plants were placed in a randomized design in two growth chambers set at 21°C day / 18°C night, 90 % relative humidity and 13-h of daylight (200 µmol m^{-2} s^{-1} photosynthetic photon fluence rate, PPFR). During this period, the plants were fertigated manually twice a day, until drainage, thus maintaining the N-treatments until the end of the experiment.

The disease was assessed by measuring the length of the lesion expanding on the stems on a daily basis. The area under the disease progress curve (AUDPC) was computed as: AUDPC = $[(Y_1/2) + \Sigma_2^{n-1} (Y_j + (Y_n/2))][I]$ where Y_j was the observed lesion (in mm) at the jth observation time, n was the total number of observations, and I the interval between each observation (in days, equal to one in our case).

Sample collection

Two-cm-long fragments of symptomless stem were collected on *Botrytis*-infected plants on each side of the lesions, approximately one cm away from the lesion margins, at 2, 4 and 7 DPI. Similar positions on the stem (between the fifth and sixth internode) were sampled from intact plants at 0 DPI and from mock-inoculated plants at 2, 4 and 7 DPI. The collected samples were immediately frozen in liquid nitrogen. Frozen stem tissues were ground into fine powder with liquid nitrogen using a mixer mills (MM301, Retsh, Haan, Germany) at a frequency of 30 Hz for 30 sec. Powders were stored in airtight pillboxes at -80°C until analysis.

The absence of RNA of fungal origin in the collected stem samples was verified by RT-qPCR as described below using a standard curve of *Botrytis* mRNA dilution in 100 ng µL^{-1} of tomato mRNA. The α-tubulin gene was used for quantification (Wu *et al.*, 2017).

9

Biochemical analyses of plant tissue

Soluble sugars (glucose, fructose and sucrose) were extracted from 10 mg of powder using a 1 mL methanol / water mixture (1:1 v/v) and 300 μL chloroform under continuous agitation. After centrifugation, 800 μL of the supernatant were evaporated under vacuum at room temperature. After the addition of 1.6 mL ultra-pure water and 10 mg PVPP, the extracts were vortexed, centrifuged and purified using a C-18 cartridge (Sep-Pak, Waters, Milford, MA, USA) and a 0.2 μm filter (Pall corporation, NY, USA). The sugars were determined by HPLC using a Sugar-Pak II pre-column and a Sugar-Pak I 300 x 6.5 mm column (Waters, Milford, MA, USA). Separation was carried out at 85°C and a flow rate of 0.6 mL min^{-1} using 50 mg L^{-1} EDTA, Na$_2$ Ca as eluent. The sugars were detected by measuring the refractive index with a RI-Detector (410, Waters, Milford, MA, USA), using the Chromelon software (ThermoFisher Scientific, Waltham, MA, USA). Sugar contents were expressed in g g^{-1} of dry weight, and relative glucose, fructose and sucrose contents (RGC, RFC and RSC, respectively) were calculated as the ratio of glucose, fructose and sucrose, respectively, to the total content of all three.

Gene expression analyses

The sequences of tomato genes involved in sucrose cleavage and sugar phosphorylation were obtained from GenBank (www.ncbi.nlm.nih.gov/genBank). A total of 31 genes were identified in the tomato genome (Supplementary data Table S1). Regarding phosphofructokinases, only predicted sequences were available, which were used to identify the corresponding genes in the tomato genome database using blast analyses (*Solanaceae* Genomics Network, www.solgenomics.net; Tomato Genome version SL4.0 and Annotation ITAG4.0). In order to verify their putative annotation, a protein sequence alignment was performed with the protein sequences of phosphofructokinase genes identified in other plants

10

(Mustroph *et al.*, 2007), using the ClustalW method with default parameters, and a phylogenetic tree was constructed (Supplementary data Fig. S1). It showed that all putative phosphofructokinases seemed valid and relevant to use.

The total RNA was isolated from 200 mg of frozen stem powder using the commercial RNeasy Plant Mini Kit (Qiagen, Hilden, Germany). To avoid DNA contamination, a DNase treatment was carried out using the RNase-Free DNase set (Qiagen, Hilden, Germany), as described by the manufacturer. The total RNA was quantified by spectrophotometry and RNA integrity quality was verified by 1% agarose gel electrophoresis.

The gene expressions were assessed by RT-qPCR. The total RNA (200 ng) was used for first strand cDNA synthesis, using oligo-$(dT)_{15}$ primers and the Reverse Transcriptase Core Kit (Eurogentec, Liège, Belgium) according to the manufacturer's instructions. The quantitative PCR (qPCR) were performed in a 384-well plate using a CFX384 cycler (Bio-Rad, Hercules, CA, USA). qPCR amplification was performed using the Takyon No Rox SYBR Core kit dTTP blue (Eurogentec, Liège, Belgium) with 1 µL of cDNA and 250 nM of forward and reverse primers and the following programme was applied: 4 min at 95°C followed by 60 cycles of 10 sec. at 95°C, and 1 min. at 60°C. To confirm the specificity of the amplicon, each qPCR programme was followed by a melting curve assay. The specific primers of targeted genes are listed in Supplementary data Table S1. Each reaction was carried out in an independent technical triplicate and included a no-template control and a reagent-only control. Quantitation cycles (Cq) were defined based on the mean of the three replicates. The geometric mean of the expression level of actin (*ACT*) and cyclophilin (*CYP*) genes was used as an internal control (reference) to normalize the expression data for the target genes. The relative expression levels of target genes were calculated as fold changes of the expression using the $2^{-\Delta\Delta Cq}$ method: 2^-[(Cq $_{(target, sample)}$ − Cq $_{(reference, sample)}$) − (Mean (Cq $_{(target, calibrator)}$ − Cq $_{(reference, calibrator)}$))] (Livak and Schmittgen, 2001), where the mean Cq values

11

corresponded to the mean of the five biological replicates. Results were $\log_2$-transformed. To assess the effect of N-treatments before inoculation, the gene expressions at 2, 10 and 20 mM NO_3^- were related to gene expressions at 0.5 mM NO_3^-. To assess the effect of infection, the gene expressions of *Botrytis*-inoculated plants were related to gene expressions of mock-inoculated plants on the same day under the respective N-treatments. Finally, to evaluate the change in gene expression over time, the gene expressions at 2, 4 and 7 days after inoculation were related to gene expressions before inoculation, under the respective N-treatments.

Statistical analyses

The data presented are the averages of five biological replicates (each in technical triplicates) ± standard error. The differences between treatments were analysed using a Kruskal-Wallis test followed by a Wilcoxon rank-sum test when necessary. All the statistical analyses were performed using R software.

RESULTS

Sufficient and over-optimal N-treatment increased fructose content and carbohydrate metabolism gene expressions before inoculation

Nitrogen availability affected the stem sugar contents before inoculation. The sucrose contents were higher, 0.046 – 0.048 g g^{-1} DW at 0.5 and 2 mM NO_3^- as compared to 0.038 g g^{-1} DW at 10 mM NO_3^- and 0.024 g g^{-1} DW at 20 mM NO_3^-. The glucose contents were around 0.062 g g^{-1} DW regardless of the N-treatment. The fructose contents were slightly lower, 0.0049 – 0.0054 g g^{-1} DW at 0.5 and 2 mM NO_3^- as compared to 0.0069 – 0.0072 g g^{-1} DW at 10 and 20 mM NO_3^- (Fig. 1A). For all N-treatments, the fructose contents were much lower than the sucrose and glucose contents. However, the relative fructose content (as

12

defined in the Materials and Methods section) increased with nitrogen availability, in parallel with a decrease in the relative sucrose content (Fig. 1B).

As the hexose-to-sucrose ratio was affected by N-treatments, we investigated the expression of genes that encode invertase, sucrose synthase, hexokinase, fructokinase and phosphofructokinase (Fig. 1C). Five among the 31 genes identified, namely *Sl-HXK6*, *Sl-FRK4*, *Sl-PFK3*, *Sl-PFK4* and *Sl-PFK7* were not expressed in the stems regardless of the condition. All invertase and sucrose synthase genes were found to be expressed in the stems. Before inoculation, most of the genes that encode sucrose cleavage enzymes, invertase and sucrose synthase showed significantly different expression levels depending on the N-treatment except for *Sl-SUS1*, *Sl-SUS4* and *Sl-NI* (Fig. 1C). Most of the relative expressions were higher at 10 and 20 mM NO_3^-. However, a threshold of ±1.5 is usually recognized as the limit for the identification of a differentiated expression, when using the $Log_2(2^{-\Delta\Delta Cq})$ relative value. Among all the genes examined, only the expression of *Sl-SUS3* at 20 mM NO_3^- reached a significantly higher mean value than this 1.5 threshold. As for the kinase encoding genes, a similar trend of higher relative expression for plants grown at 10 and 20 mM NO_3^- was noted, but the differences were only significant for *Sl-HXK1* and *Sl-FRK3*.

Disease severity decreased with high relative fructose content before inoculation

Four weeks after the beginning of the N-treatments, the plants were inoculated with *B. cinerea* and incubated during seven days. The petiole stubs were colonized and lesions developed on the stems within 72 − 96h. The AUDPC was computed based on the measurement of lesion lengths between 4 and 7 days post inoculation (DPI). As expected based on previous studies, N-treatments affected plant susceptibility (p = 0.0003, Fig. 2A) with a more than threefold difference in AUDPC for plants grown with 0.5 mM NO_3^- in the nutrient solution and those grown with 10 mM NO_3^-, and no difference between plants grown

13

with 10 and 20 mM NO_3^-. We observed a tight curvilinear relationship between RFC before inoculation and AUDPC (Fig. 2B), while no significant results could be obtained when trying to fit various functions into the relationship between RSC and AUDPC, RGC and AUDPC, or plant nitrate content and AUDPC.

Susceptible plants accumulated fructose after the onset of the infection under low N-treatment

To ensure favourable incubation and regular disease development after leaf pruning, plants were transferred from a glasshouse to growth chambers, with an adjustment of the air temperature, its relative humidity and the light intensity. Consequently, the sugar metabolism was affected both in *Botrytis*-inoculated and mock-inoculated plants after this transfer (Fig. 3).

The sugar contents were analysed after confirmation by qPCR of the absence of *Botrytis* in asymptomatic regions of stems surrounding the lesions. We observed that N-treatments affected soluble sugar contents at all sampling dates after inoculation (Fig. 3). Under sufficient and over-optimal N-treatments (10 and 20 mM NO_3^-), no differences between *Botrytis* and mock-inoculated plants were observed. Fructose and glucose contents decreased between 0 and 7 DPI. Sucrose content dropped between 0 and 2 DPI, and remained roughly constant thereafter at 10 mM NO_3^-, while at 20 mM NO_3^- it remained constant between 0 and 4 DPI, and slightly increased between 4 and 7 DPI. Contrasts between *Botrytis*-inoculated and mock-inoculated plants were much more pronounced under low N-treatment. Fructose and glucose contents initially decreased after inoculation with *Botrytis*, but while glucose showed no significant evolution between 2 and 7 DPI, fructose started to accumulate between 2 and 4 DPI at 0.5 mM NO_3^-, and 4 DPI at 2 mM NO_3^-. An opposite pattern was observed in mock-inoculated plants, with an initial rise of glucose and fructose

14

contents, followed by a decrease at 2 DPI. The sucrose content of infected plants started to drop at 4 DPI, while that of mock-inoculated plants started to decrease earlier, at 2 DPI. Thus, the major difference observed between infected and mock-inoculated plants was the accumulation of fructose in infected plants in the low N-treatments.

Botrytis *infection affected the expression of genes that encode sucrose cleavage enzymes*

The expression of genes involved in sugar metabolism after inoculation were examined. The expressions of sugar metabolism genes in *Botrytis*-inoculated plants relative to those of mock-inoculated plants measured on the same day (y axis) as well as the gene expressions of inoculated plants relative to those measured before inoculation (x axis) were plotted in fig. 4 for sucrose cleaving enzymes. The gene expressions that exceed the ± 1.5 threshold of ΔΔCq are highlighted in Figs 4 and 5. Graphs that compare individual gene expressions under the four N-treatments and the related statistics are provided in Supplementary data Fig. S2.

N-treatments strongly affected gene expressions after inoculation, especially at 2 DPI (Supplementary data Fig. S2). Two groups of sucrose synthases may be distinguished. On the one hand, *Botrytis* inoculation stimulated the expression of *Sl-SUS1* and *Sl-SUS3* at 2 DPI, but the transcript levels (relative to those of mock-inoculated plants) were much higher for plants grown at 10 and 20 mM NO_3^- than for plants grown at lower N levels (Fig. 4, Supplementary data Fig. S2A). When related to their levels of expression before inoculation, *Sl-SUS1* and *Sl-SUS3* were stimulated by the infection under all N-treatments, however more strongly under high N-treatment (Fig. 4). On the other hand, a second group of transcripts, corresponding to *Sl-SUS4* to *Sl-SUS7* were lower at 0.5 and 2 mM NO_3^-, relative to mock-inoculated plants, whereas no such repression was detected at higher NO_3^- concentrations. A similar contrast was observed for invertases. The relative expressions of *Sl-LIN5*, *Sl-LIN7*, *Sl-*

LIN8, *Sl-LIN9* and *Sl-VI* were negative at 0.5 and 2 mM NO_3^- and positive at 10 and 20 mM NO_3^- (Fig. 4, Supplementary data Fig. S2A). *Sl-LIN6* showed a particular pattern, since its relative expression was high regardless of the N-treatment, though it increased from 2.5 at 0.5 mM NO_3^- to 5 at 20 mM NO_3^-. The gene that encoded the *Sl-NI* mitochondrial invertase hardly showed any variation after inoculation, regardless of the N-treatment. The observed contrasts of relative expressions according to N-treatments were attenuated at 4 and 7 DPI (Supplementary data Fig. S2B,C). Relative to mock-inoculated plants, *Sl-SUS1* and *Sl-SUS3* transcripts were higher under low N-treatments, especially at 7 DPI, while *Sl-SUS4* to *Sl-SUS7* were still repressed at 0.5 mM NO_3^-, and to a lesser extent at 2 mM NO_3^- (Supplementary data Fig S2C). The *Sl-LIN5*, *Sl-LIN7*, *Sl-LIN8* and *Sl-VI* invertases were still repressed, in comparison with mock-inoculated plants, at 4 DPI, but not at 7 DPI. By contrast, *Sl-LIN6* and *Sl-LIN9* were strongly expressed at 4 and 7 DPI, with higher transcript levels under low N-treatments. To summarize, *Sl-SUS1* and *Sl-SUS3* were activated upon infection, and the early activation of these genes as well as those that encode cell wall invertases were associated with reduced susceptibility, while on the contrary, the early repression of *Sl-SUS4* to *Sl-SUS7* and cell wall invertases, except for *Sl-LIN6*, was associated with increased susceptibility.

Botrytis *infection affected hexose kinase gene expressions*

Similarly to genes that encode sucrose cleavage enzymes, several genes that encode hexose kinases showed contrasted expressions two days after inoculation, depending on the N-treatment. *Sl-HXK1*, *Sl-FRK1* to *Sl-FRK3*, *Sl-PFK1* and to a lesser extent *Sl-HXK2* and *Sl-HXK5* showed enhanced expressions at 10 and 20 mM NO_3^-, relative to mock-inoculated plants (Fig. 5, Supplementary data Fig. S2A). In contrast, *Sl-HXK5* and *Sl-FRK3* were repressed at 0.5 and 2 mM NO_3^-. The putative phosphofructokinase gene *Sl-PFK6* was strongly activated under all N-treatments, relative to the expression in mock-inoculated

16

plants, and relative to its expression level before inoculation. Differences between N-treatments were much less pronounced at 4 DPI (Supplementary data Fig. S2B), at which time the transcript levels of *Sl-HXK5*, *Sl-FRK1* to *Sl-FRK3*, *Sl-PFK1*, *Sl-PFK2*, *Sl-PFK5*, *Sl-PFK6* and *Sl-PFK8* were lower in *Botrytis*-inoculated plants in comparison with mock-inoculated ones regardless of the N-treatments. At 7 DPI, the relative expression of hexose kinases was very low, regardless of the N-treatments. Thus, the condition of reduced susceptibility was associated with an activation of all fructokinases genes, along with *Sl-HXK1*, *Sl-HXK2* and *Sl-HXK5* hexokinases and the *Sl-PFK1* phosphofructokinase. Conversely, the condition of enhanced susceptibility was associated with a repression of *Sl-HXK5* and *Sl-FRK3*.

DISCUSSION

In the present work, we used contrasted N-treatments to examine the sugar metabolism associated with the increased resistance or susceptibility of tomato stems to *B. cinerea*. We analysed the content of soluble sugars (sucrose, glucose and fructose) and the expression of genes involved in the catabolism of sucrose and the first phosphorylating steps of glycolysis. The metabolites and transcript levels were quantified in symptomless stem tissues surrounding *Botrytis* lesions. Stems are sink tissues for which little is known regarding the relationship between sugars and the response to infection. The particularity of sink tissues lies in the activity of sucrose synthase, generally not perceived in source tissues (Wind *et al.*, 2010). Among the 31 genes of invertases, sucrose synthases, hexokinases, fructokinases and phosphofructokinases analysed in this work (Supplementary data Table S1), we detected the expression of 26 genes. All sucrose synthase and invertase genes are expressed in tomato stems, *Sl-SUS1*, *Sl-SUS3*, *Sl-SUS5*, *Sl-LIN8* and *Sl-VI* being the most abundant isoforms, according to Hyun *et al.* (2011) and Qin *et al.* (2016). Fructokinase genes *Sl-FRK1* to *Sl-FRK3* are expressed in all vascular tissues unlike *Sl-FRK4* which is specific to anthers and

17

pollen (German *et al.*, 2002; Granot *et al.*, 2013; Stein *et al.*, 2018) and, accordingly, was not detected in this study. We did not record transcripts of the *Sl-HXK6* hexokinase gene and of the *Sl-PFK3*, *Sl-PFK4* and *Sl-PFK7* putative phosphofructokinase genes; it can be hypothesized that these genes are not expressed in tomato stems. The main objective of gene expression analysis was to compare the transcriptional activity of wounded and mock-inoculated plants with wounded and *Botrytis*-inoculated plants, under various N-treatments. Knowing that the expression levels of the genes studied are not quantitatively linked to their enzymatic activity (Keurentjes *et al.*, 2008), and that the metabolic transformation of sugars relies on multiple reversible reactions, the relationship between gene expression and sugar content observed in this work may only indicate a qualitative defence response induced by the various N-treatment. Moreover, a leaf was cut off in order to carry out both the mock-inoculation and the *Botrytis*-inoculation. In a study on *Arabidopsis*, a modification in the expression of the *AtC/VIF2* gene, which encodes a cell-wall invertase inhibitor, was measured following an infiltration for a mock-inoculation (Bonfig *et al.*, 2010). This may indicate the possible effect of wounding on invertase activity unrelated to the pathogen infection. For all these reasons, the gene expression of *Botrytis*-inoculated plants presented here were expressed relatively to those of mock-inoculated plants.

We initially analysed the effect of N-treatments on constitutive gene expressions and sugar contents before inoculation. These treatments mostly affected sucrose content, which was twice as high at 0.5 and 2 mM NO_3^- compared to 20 mM NO_3^-. In the tomato cultivar used in this work, the fructose content was much lower than the glucose content, and slightly lower under low N-treatments. Other studies have described higher sucrose and total reducing sugars contents in sink tissues under nitrogen stress (Cazetta *et al.*, 1999; Krapp *et al.*, 2011). Most probably, sucrose (and starch) accumulation may be linked to reduced growth at low nitrogen levels. Accordingly, in this study we found that several, but not all isoforms of cell

18

wall invertases and sucrose synthases showed reduced expression levels under low N-treatments. A reduced activity of invertases at low nitrogen availability has been shown in cassava leaves (Cruz *et al.*, 2003) and maize kernels (Cazetta *et al.*, 1999).

Many reports, regularly reviewed in the past decade, have emphasized the role of host sugars and related enzymes in plant-pathogen interactions (Bolton, 2009; Bolouri Moghaddam and Van den Ende, 2012; Tauzin and Giardina, 2014; Kanwar and Jha, 2019). The plant nitrogen status is known to affect disease incidence and development in multiple ways (Fagard *et al.*, 2014), and nitrogen nutrition has already proved to be a modulator of *Botrytis* susceptibility in tomato leaves and fruit (Vega *et al.*, 2015) as well as stems (Lecompte *et al.*, 2017). Plant infection by pathogens is known to induce a massive reprogramming of the host cell machinery from growth to defence. This takes place via the inhibition of photosynthesis at infection sites in photosynthetic tissues, and the coincident activation of sugar transporters and sucrose-cleaving enzymes, the modulation of the carbohydrate metabolism and hexose-to-sucrose ratio, and the production of end products of hexose metabolism, *e.g.* cell wall compounds (Bellincampi *et al.*, 2014), hormones (Beyers *et al.*, 2014) and antimicrobial compounds (Tiku, 2018). It has been suggested that high levels of soluble sugars in the host generally favour plant resistance to pathogens (Morkunas and Ratajczak, 2014). Accordingly, in one study by Hoffland *et al.* (1999), tomato leaf susceptibility to *B. cinerea* was positively correlated with the soluble carbohydrates content. However this was not the case in lettuce leaves (Lecompte *et al.*, 2013), and tomato stems, as shown in the present study and in previous work (Lecompte *et al.*, 2017). The effect of elevated N-treatments on reduced tomato stem susceptibility to *B. cinerea* is not correlated, whether positively or negatively, with the total content of soluble sugars. Instead, a strong and robust correlation between stem susceptibility and the constitutive relative fructose content has been shown in previous studies (Lecompte *et al.*, 2017) and in the present one. In

19

this study, we have observed an early accumulation of hexoses in mock-inoculated plants grown under low N-treatments. By contrast, a rise in fructose content was observed later (between 2 and 4 DPI) in infected plants under low N-treatments. Regarding mock-inoculated plants, the observed hexose accumulation may have been due to leaf pruning and the environmental changes associated to the transfer of plants in the growth chamber. However, nitrogen nutrition interfered with the response since no hexose accumulation was observed under high N-treatments. Regarding *Botrytis*-inoculated plants, under low N-treatments, the late accumulation of fructose might be related to the lower expression of hexokinases and fructokinases observed. Thus, under low N-treatments, less fructose might be involved in the glycolysis and further synthesis of defence compounds. However, since the measurements were performed in tissues neighbouring the lesions, it could also be hypothesized that hexoses were not used in these asymptomatic cells, and rather remobilized in sucrose and then transported to the infection site. Studying the host sugar dynamics in tissues colonized with fungal mycelium is complex, since the retrieval of host sugars by the pathogen must be estimated using specific labelling techniques (Dulermo *et al.*, 2009).

In the present work, the inoculation of *B. cinerea* triggered a high and early transcription of all isoforms of invertases, as well as *Sl-SUS1* and *Sl-SUS3*, under the N-treatments which provided 10 and 20 mM NO_3^- in the nutrient solution, and this transcriptional activity was associated with phenotypes with reduced susceptibility. By contrast, more susceptible plants displayed repressed expressions of *Sl-SUS4* to *Sl-SUS7* and of some invertase isoform genes under low N-treatments. Interestingly, nitrogen availability affected the constitutive expression of *Sl-SUS3* before and after infection, while the over-expression of *Sl-SUS1* was only observable after infection. *Sl-SUS3* expression in healthy tomato plants is mostly associated to vascular tissues and changes according to stem maturity (Goren *et al.*, 2011). In our work, the over-expression, before infection, of *Sl-SUS3* at

20

sufficient (10 mM) and over-optimal (20 mM) nitrogen availability could correspond to the higher stem volumes observed in these treatments. However, the over-expression of *Sl-SUS1* is both dependent on infection and high nitrogen availability. Here we highlight the conditional involvement of some specific isoforms of sucrose synthases in a successful defence.

The *Sl-LIN6* invertase was over-expressed in all N-treatments along the course of infection. In leaves of tomato and *Arabidopsis* infected by *B. cinerea*, *Sl-LIN6* (Berger *et al.*, 2004) and *At-CWIN1* (Veillet *et al.*, 2016) invertases are activated. In addition, an increased apoplastic hexose uptake and an up-regulation of several sugar transporter genes have been observed after infection by *B. cinerea* (Lemonnier *et al.*, 2014; Veillet *et al.*, 2017; Bezrutczyk *et al.*, 2018). The internalization of sugars may participate in "pathogen starvation", a defence mechanism that potentially limits the availability of apoplastic sugar for the pathogen (Bezrutczyk *et al.*, 2018). However, in this work, an increased expression of genes that encode sucrose synthases, which have a cytosolic activity, was observed after inoculation. This strengthens the hypothesis of a higher recruitment of hexoses by the host tissues. Oppositely, the down-regulation of some invertases in susceptible plants may facilitate the maintenance of elevated apoplastic sucrose availability, in favour of the pathogen.

Less susceptible plants observed in this work up-regulated the transcription of sugar metabolism genes two days after inoculation. Several studies have already highlighted the importance of the early stage response for increased resistance (Hyun *et al.*, 2011; Birkenbihl *et al.*, 2012; De Cremer *et al.*, 2013). In this work, susceptible plants showed delayed expressions of *Sl-SUS1*, *Sl-SUS3*, *Sl-LIN8* and *Sl-LIN9* along with the continuous repression of several *Sl-SUS4* to *Sl-SUS7* isoforms throughout the course of infection. This repression of sucrose cleavage enzymes was associated to poorly effective defence. It originated from the

21

low host nitrogen status, but whether the fungus is able to manipulate this expression in a nitrogen-dependent manner remains to be examined.

Hexokinases are known to be involved in plant / pathogen interaction (Morkunas and Ratajczak, 2014; Rojas *et al.*, 2014), but fructokinase and phosphofructokinase gene expressions after infection by a necrotrophic fungus have not been described thoroughly in the literature. Here, more susceptible plants showed repressed fructokinase transcript levels, in comparison with mock-inoculated plants, while more resistant plants under sufficient and over-optimal N-treatments showed higher levels of transcripts of *Sl-FRK1* to *Sl-FRK3* early after inoculation. In accordance with lower fructokinase transcript levels, higher levels of fructose contents were observed at low nitrogen availability, thus suggesting a lower mobilization of fructose for the glycolysis. A similar accumulation of fructose in tomato stems after infection at low nitrogen availability has already been observed in another tomato cultivar (Lecompte *et al.*, 2017).

Recent work on metabolomics and transcriptomics highlighted cell wall reinforcement with callose, and lignins, as a successful strategy against *B. cinerea* (Asselbergh *et al.*, 2007; Curvers *et al.*, 2010; Yang *et al.*, 2018). Sucrose synthase cleaves sucrose into fructose and UDP-glucose, the latter being presumed to trigger cell wall reinforcement. The early expression of fructokinase genes in resistant plants observed in this study suggests that the activity of sucrose synthase may not be limited to cell wall reinforcement, unless fructose catabolism in the glycolysis is a fortuitous consequence of defence activation. However, others works suggest that glycolysis and subsequent pathways are useful for defence (Agudelo-Romero *et al.*, 2015; Camañes *et al.*, 2015; AbuQamar *et al.*, 2016). On the one hand, the GS / GOGAT activity and the assimilation of nitrogen may control, away from sugar regulation, the maintenance of cell homeostatis against pathogenic fungi (Seifi *et al.*, 2013). On the other hand, the pentose phosphate pathway supports the

22

synthesis of precursors of phenylpropanoid compounds which are synthesized in response to *B. cinerea* (Ma *et al.*, 2018). Thus, the supplemental fructose synthesis from sucrose synthase activity, followed by its phosphorylation and entry into the glycolysis may be needed for increased resistance in sink tissues.

In conclusion, this study shows that the increased resistance of tomato stem to *B. cinerea* is supported by an early activation of genes that encode sucrose cleavage enzymes: invertases and sucrose synthases. This is only observed in conditions of sufficient or over-optimal nitrogen availability. By contrast, in conditions of low nitrogen availability, an early repression of several sucrose synthase and invertase genes is observed after infection. The cytosolic activity of sucrose synthase associated with the enhanced expression of hexokinases and fructokinases in resistant plants support the hypothesis of an increased synthesis of cell wall components and / or the recruitment of additional fructose in glycolysis and subsequent pathways for an effective defence.

23

ACKNOWLEDGEMENTS

LITERATURE CITED

AbuQamar SF, Moustafa K, Tran L-SP. 2016. 'Omics' and Plant Responses to *Botrytis cinerea*. *Frontiers in Plant Science* **7**: 1–8.

Agudelo-Romero P, Erban A, Rego C, *et al.* 2015. Transcriptome and metabolome reprogramming in *Vitis vinifera* cv. Trincadeira berries upon infection with *Botrytis cinerea*. *Journal of Experimental Botany* **66**: 1769–1785.

Aguilera-Alvarado GP, Sanchez-Nieto S. 2017. Plant Hexokinases are Multifaceted Proteins. *Plant and Cell Physiology* **58**: 1151–1160.

Asselbergh B, Curvers K, França SC, *et al.* 2007. Resistance to *Botrytis cinerea* in sitiens, an abscisic acid-deficient tomato mutant, involves timely production of hydrogen peroxide and cell wall modifications in the epidermis. *Plant Physiology* **144**: 1863–1877.

Bellincampi D, Cervone F, Lionetti V. 2014. Plant cell wall dynamics and wall-related susceptibility in plant-pathogen interactions. *Frontiers in Plant Science* **5**: 1–8.

Berger S, Papadopoulos M, Schreiber U, Kaiser W, Roitsch T. 2004. Complex regulation of gene expression, photosynthesis and sugar levels by pathogen infection in tomato. *Physiologia Plantarum* **122**: 419–428.

Berger S, Sinha AK, Roitsch T. 2007. Plant physiology meets phytopathology: Plant primary metabolism and plant-pathogen interactions. *Journal of Experimental Botany* **58**: 4019–4026.

Beyers T, Vos C, Aerts R, *et al.* 2014. Resistance against Botrytis cinerea in smooth leaf pruning wounds of tomato does not depend on major disease signalling pathways. *Plant Pathology* **63**: 165–173.

25

Bezrutczyk M, Yang J, Eom JS, *et al.* 2018. Sugar flux and signaling in plant–microbe interactions. *Plant Journal* **93**: 675–685.

Birkenbihl RP, Diezel C, Somssich IE. 2012. *Arabidopsis* WRKY33 Is a Key Transcriptional Regulator of Hormonal and Metabolic Responses toward *Botrytis cinerea* Infection. *Plant Physiology* **159**: 266–285.

Bolouri Moghaddam MR, Van den Ende W. 2012. Sugars and plant innate immunity. *Journal of Experimental Botany* **63**: 3989–3998.

Bolton MD. 2009. Primary Metabolism and Plant Defense—Fuel for the Fire. *Molecular Plant-Microbe Interactions* **22**: 487–497.

Bonfig KB, Gabler A, Simon UK, *et al.* 2010. Post-translational derepression of invertase activity in source leaves via down-regulation of invertase inhibitor expression is part of the plant defense response. *Molecular Plant* **3**: 1037–1048.

Brzin J, Petrovič N, Ravnikar M, Kovač M. 2011. Induction of sucrose synthase in the phloem of phytoplasma infected maize. *Biologia Plantarum* **55**: 711–715.

Cabello S, Lorenz C, Crespo S, *et al.* 2014. Altered sucrose synthase and invertase expression affects the local and systemic sugar metabolism of nematode-infected *Arabidopsis thaliana* plants. *Journal of Experimental Botany* **65**: 201–212.

Camañes G, Scalschi L, Vicedo B, González-Bosch C, García-Agustín P. 2015. An untargeted global metabolomic analysis reveals the biochemical changes underlying basal resistance and priming in *Solanum lycopersicum*, and identifies 1-methyltryptophan as a metabolite involved in plant responses to *Botrytis cinerea* and *Pseudomonas sy*. *Plant Journal* **84**: 125–139.

Cazetta JO, Seebauer JR, Below FE. 1999. Sucrose and nitrogen supplies regulate growth of maize kernels. *Annals of Botany* **84**: 747–754.

Chen LQ, Hou BH, Lalonde S, *et al.* 2010. Sugar transporters for intercellular exchange and nutrition of pathogens. *Nature* **468**: 527–532.

De Cremer K, Mathys J, Vos C, *et al.* 2013. RNAseq-based transcriptome analysis of *Lactuca sativa* infected by the fungal necrotroph *Botrytis cinerea*. *Plant, Cell and Environment* **36**: 1992–2007.

Cruz JL, Mosquim PR, Pelacani CR, Araújo WL, DaMatta FM. 2003. Carbon partitioning and assimilation as affected by nitrogen deficiency in cassava. *Photosynthetica* **41**: 201–207.

Curvers K, Seifi H, Mouille G, *et al.* 2010. Abscisic acid deficiency causes changes in cuticle permeability and pectin composition that influence tomato resistance to *Botrytis cinerea*. *Plant Physiology* **154**: 847–860.

Dulermo T, Rascle C, Chinnici G, Gout E, Bligny R, Cotton P. 2009. Dynamic carbon transfer during pathogenesis of sunflower by the necrotrophic fungus Botrytis cinerea: From plant hexoses to mannitol. *New Phytologist* **183**: 1149–1162.

Fagard M, Launay A, Clément G, *et al.* 2014. Nitrogen metabolism meets phytopathology. *Journal of Experimental Botany* **65**: 5643–5656.

Fatima U, Senthil-Kumar M. 2015. Plant and pathogen nutrient acquisition strategies. *Frontiers in Plant Science* **6**: 1–12.

Fotopoulos V, Gilbert MJ, Pittman JK, *et al.* 2003. The Monosaccharide Transporter Gene. *Society* **132**: 821–829.

27

Fotopoulos V. 2005. Plant invertases : structure, function and regulation. *Journal of Biological Research* **4**: 127–137.

German MA, Dai N, Chmelnitsky I, *et al.* **2002.** LeFRK4, a novel tomato (*Lycopersicon esculentum* Mill.) fructokinase specifically expressed in stamens. *Plant Science* **163**: 607–613.

Glazebrook J. 2005. Contrasting Mechanisms of Defense Against Biotrophic and Necrotrophic Pathogens. *Annual Review of Phytopathology* **43**: 205–227.

Goren S, Huber SC, Granot D. 2011. Comparison of a novel tomato sucrose synthase, *SlSUS4*, with previously described *SlSUS* isoforms reveals distinct sequence features and differential expression patterns in association with stem maturation. *Planta* **233**: 1011–1023.

Granot D. 2007. Role of tomato hexose kinases. *Functional Plant Biology* **34**: 564–570.

Granot D, David-Schwartz R, Kelly G. 2013. Hexose kinases and their role in sugar-sensing and plant development. *Frontiers in Plant Science* **4**: 1–17.

Hoffland E, Van Beusichem ML, Jeger MJ. 1999. Nitrogen availability and susceptibility of tomato leaves to Botrytis cinerea. *Plant and Soil* **210**: 263–272.

Hren M, Ravnikar M, Brzin J, *et al.* **2009.** Induced expression of sucrose synthase and alcohol dehydrogenase I genes in phytoplasma-infected grapevine plants grown in the field. *Plant Pathology* **58**: 170–180.

Hyun TK, Eom SH, Rim Y, Kim J. 2011. Alteration of the expression and activation of tomato invertases during *Botrytis cinerea* infection. *Plant Omics* **4**: 413–417.

Kanwar P, Jha G. 2019. Alterations in plant sugar metabolism: signatory of pathogen attack. *Planta* **249**: 305–318.

28

Keurentjes JJB, Sulpice R, Gibon Y, et al. 2008. Integrative analyses of genetic variation in enzyme activities of primary carbohydrate metabolism reveal distinct modes of regulation in Arabidopsis thaliana. *Genome Biology* **9**: 1–20.

Krapp A, Berthomé R, Orsel M, *et al.* 2011. *Arabidopsis* roots and shoots show distinct temporal adaptation patterns toward nitrogen starvation. *Plant Physiology* **157**: 1255–1282.

Lecompte F, Abro MA, Nicot PC. 2010. Contrasted responses of *Botrytis cinerea* isolates developing on tomato plants grown under different nitrogen nutrition regimes. *Plant Pathology* **59**: 891–899.

Lecompte F, Abro MA, Nicot PC. 2013. Can plant sugars mediate the effect of nitrogen fertilization on lettuce susceptibility to two necrotrophic pathogens: *Botrytis cinerea* and *Sclerotinia sclerotiorum*? *Plant and Soil* **369**: 387–401.

Lecompte F, Nicot PC, Ripoll J, *et al.* 2017. Reduced susceptibility of tomato stem to the necrotrophic fungus *Botrytis cinerea* is associated with a specific adjustment of fructose content in the host sugar pool. *Annals of Botany* **119**: 931–943.

Lemonnier P, Gaillard C, Veillet F, *et al.* 2014. Expression of *Arabidopsis* sugar transport protein STP13 differentially affects glucose transport activity and basal resistance to *Botrytis cinerea*. *Plant Molecular Biology* **85**: 473–484.

Livak KJ, Schmittgen TD. 2001. Analysis of relative gene expression data using real-time quantitative PCR and the 2-ΔΔCT method. *Methods* **25**: 402–408.

Lopez J, Tremblay N, Voogt W, Dubé S, Gosselin A. 1996. Effects of varying sulphate concentrations on growth, physiology and yield of the greenhouse tomato. *Scientia Horticulturae* **67**: 207–217.

Ma L, He J, Liu H, Zhou H. 2018. The phenylpropanoid pathway affects apple fruit resistance to *Botrytis cinerea*. *Journal of Phytopathology* **166**: 206–215.

Morkunas I, Ratajczak L. 2014. The role of sugar signaling in plant defense responses against fungal pathogens. *Acta Physiologiae Plantarum* **36**: 1607–1619.

Mustroph A, Sonnewald U, Biemelt S. 2007. Characterisation of the ATP-dependent phosphofructokinase gene family from *Arabidopsis thaliana*. *FEBS Letters* **581**: 2401–2410.

Oliva R, Quibod IL. 2017. Immunity and starvation: new opportunities to elevate disease resistance in crops. *Current Opinion in Plant Biology* **38**: 84–91.

Paulina Aguilera-Alvarado G, Sanchez-Nieto S. 2017. Plant Hexokinases are Multifaceted Proteins. *Plant and Cell Physiology* **58**: 1151–1160.

Pego J V., Smeekens SCM. 2000. Plant fructokinases: A sweet family get-together. *Trends in Plant Science* **5**: 531–536.

Proels RK, Hückelhoven R. 2014. Cell-wall invertases, key enzymes in the modulation of plant metabolism during defence responses. *Molecular Plant Pathology* **15**: 858–864.

Qin G, Zhu Z, Wang W, *et al.* 2016. A Tomato Vacuolar Invertase Inhibitor Mediates Sucrose Metabolism and Influences Fruit Ripening. *Plant Physiology* **172**: 1596–1611.

Rios JA, Rios VS, Aucique-Pérez CE, *et al.* 2017. Alteration of photosynthetic performance and source–sink relationships in wheat plants infected by *Pyricularia oryzae*. *Plant Pathology* **66**: 1496–1507.

Rojas CM, Senthil-Kumar M, Tzin V, Mysore KS. 2014. Regulation of primary plant metabolism during plant-pathogen interactions and its contribution to plant defense. *Frontiers in Plant Science* **5**: 1–12.

Ruan Y-L. 2014. Sucrose Metabolism: Gateway to Diverse Carbon Use and Sugar Signaling. *Annual Review of Plant Biology* **65**: 33–67.

Sarowar S, Lee JY, Ahn ER, Pai HS. 2008. A role of hexokinases in plant resistance to oxidative stress and pathogen infection. *Journal of Plant Biology* **51**: 341–346.

Seifi HS, Van Bockhaven J, Angenon G, Höfte M. 2013. Glutamate Metabolism in Plant Disease and Defense: Friend or Foe? *Molecular Plant-Microbe Interactions* **26**: 475–485.

Stein O, Damari-Weissler H, Secchi F, *et al.* 2016. The tomato plastidic fructokinase *SlFRK3* plays a role in xylem development. *New Phytologist* **209**: 1484–1495.

Stein O, Granot D. 2018. Plant fructokinases: Evolutionary, developmental, and metabolic aspects in sink tissues. *Frontiers in Plant Science* **9**: 1–12.

Stein O, Granot D. 2019. An overview of sucrose synthases in plants. *Frontiers in Plant Science* **10**: 1–14.

Stein O, Secchi F, German MA, *et al.* 2018. The tomato cytosolic fructokinase FRK1 is important for phloem fiber development. *Biologia Plantarum* **62**: 353–361.

Tauzin AS, Giardina T. 2014. Sucrose and invertases, a part of the plant defense response to the biotic stresses. *Frontiers in Plant Science* **5**: 1–8.

Tiku AR. 2018. Antimicrobial compounds and their role in plant defense. *Molecular Aspects of Plant-Pathogen Interaction* **13**: 283–307.

Vega A, Canessa P, Hoppe G, *et al.* 2015. Transcriptome analysis reveals regulatory networks underlying differential susceptibility to *Botrytis cinerea* in response to nitrogen availability in *Solanum lycopersicum. Frontiers in Plant Science* **6**: 1–17.

31

Veillet F, Gaillard C, Coutos-Thévenot P, La Camera S. 2016. Targeting the *AtCWIN1* Gene to Explore the Role of Invertases in Sucrose Transport in Roots and during *Botrytis cinerea* Infection. *Frontiers in Plant Science* **7**: 1–20.

Veillet F, Gaillard C, Lemonnier P, Coutos-Thévenot P, La Camera S. 2017. The molecular dialogue between *Arabidopsis thaliana* and the necrotrophic fungus *Botrytis cinerea* leads to major changes in host carbon metabolism. *Scientific Reports* **7**: 1–13.

Wind J, Smeekens S, Hanson J. 2010. Sucrose: Metabolite and signaling molecule. *Phytochemistry* **71**: 1610–1614.

Windram O, Madhou P, Mchattie S, *et al.* 2012. *Arabidopsis* defense against *Botrytis cinerea*: Chronology and regulation deciphered by high-resolution temporal transcriptomic analysis. *Plant Cell* **24**: 3530–3557.

Wu X, Yang H, Ren H, *et al.* 2017. Selection of reliable reference genes for gene expression studies in *Botrytis cinerea*. *Journal of Microbiological Methods* **142**: 71–75.

Yang C, Liang Y, Qiu D, Zeng H, Yuan J, Yang X. 2018. Lignin metabolism involves *Botrytis cinerea* BcGs1- induced defense response in tomato. *BMC Plant Biology* **18**: 1–15.

32

LEGENDS TO FIGURES

FIG. 1: Carbohydrate metabolism status of tomato stems according to N-treatment prior inoculation. Sugar contents (A) and relative sugar contents (RSC, RGC and RFC for sucrose, glucose and fructose respectively) (B) before inoculation are plotted according to the N-treatment. Each bar is the mean ± standard error of five observations, corresponding to five plants per N-treatment, one observation per plant. Letters above symbols indicate significant differences between N-treatments according to a Wilcoxon rank-sum, one test per sugar. Relative gene expression (C) was calculated using the $\log_2(2^{-\Delta\Delta Cq})$ formula with *Sl-ACT* and *Sl-CYP* as a control for normalization. The mean of five observations (corresponding to five plants per N-treatment, one observation per plant) was computed. Asterisks beside gene names indicate the levels of significance according to N-treatments (Kruskal-Wallis test, ** when $0.001 < P < 0.01$ and * when $0.01 < P < 0.05$).
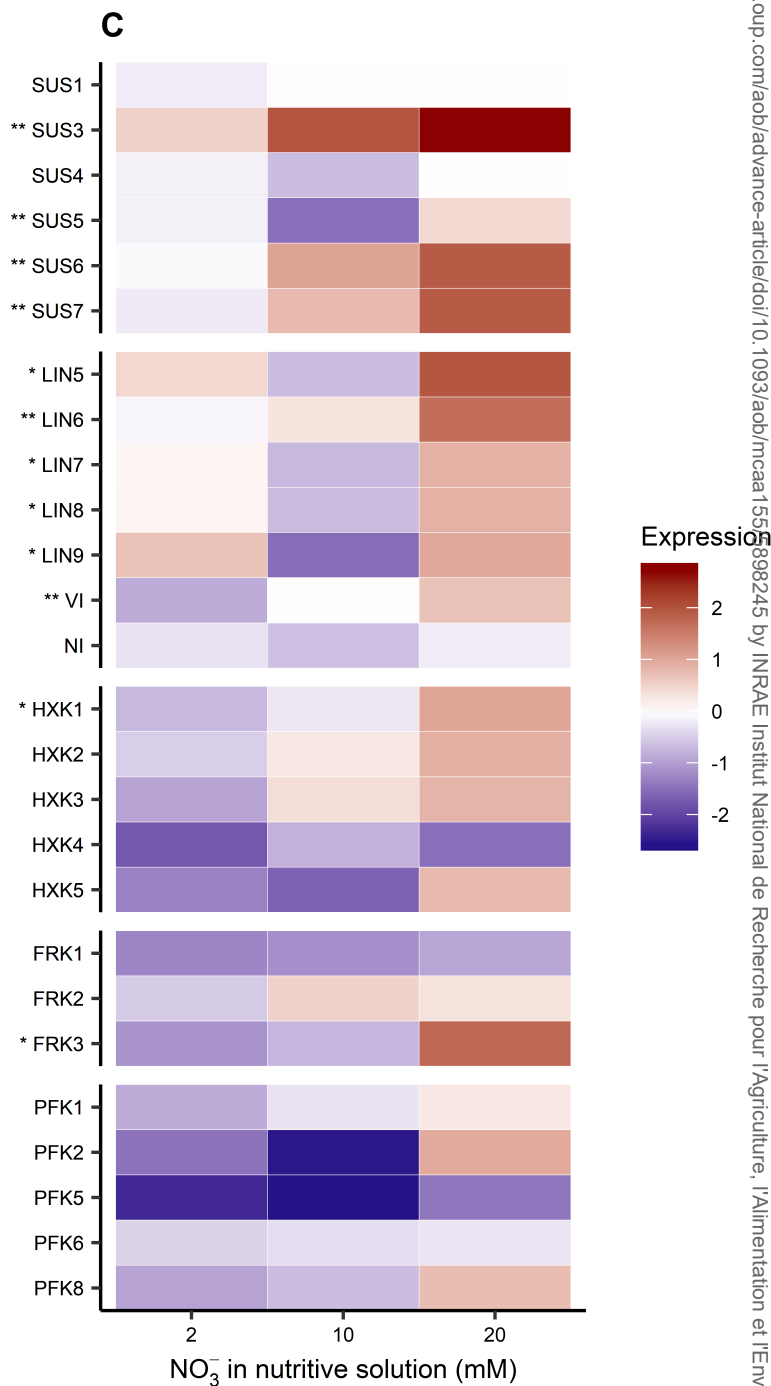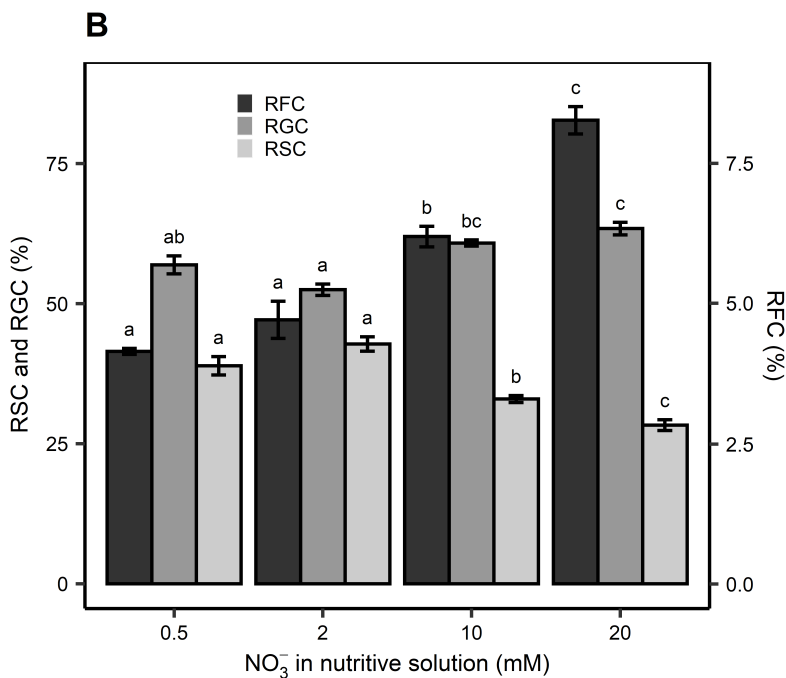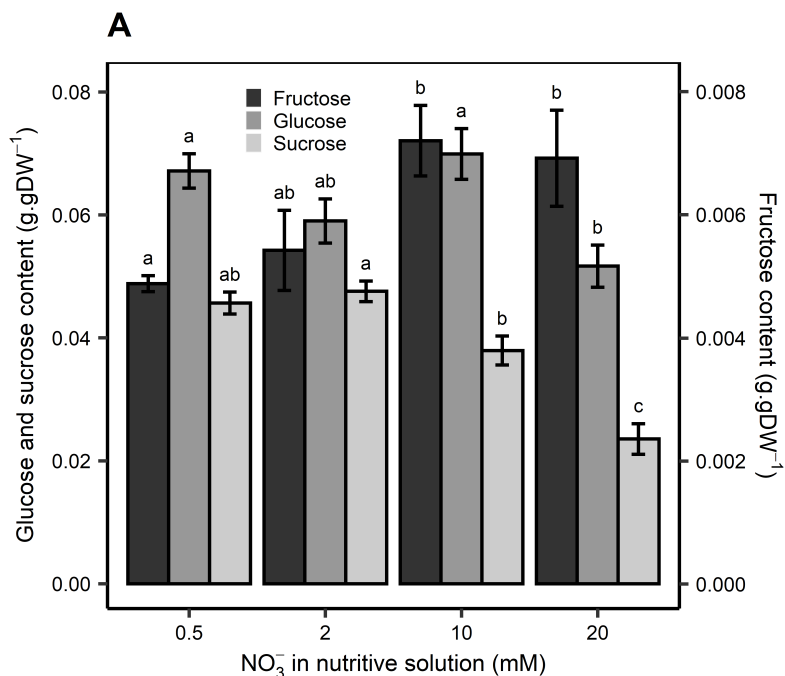
FIG. 2: Relationship between disease severity, N-treatment and carbohydrate metabolism. (A) Average values of area under the disease progress curve (AUDPC) on tomato stems under four N-treatment. Each bar is the mean ± standard error of five observations (corresponding to five plants per N-treatment, one observation per plant). Letters above symbols indicate significant differences between N-treatments according to a Wilcoxon rank-sum test. (B) Relationship between the AUDPC and relative fructose content (RFC) of the tomato stem before inoculation. Each symbol corresponds to the mean ± standard error of five observations (corresponding to five plants per N-treatment, one observation per plant).

FIG. 3: Evolution of sugar contents after *Botrytis* inoculation in fungus-free tomato stems. Closed circles with full lines correspond to mock-inoculated plant and open circles with dotted lines correspond to *Botrytis*-inoculated plants. Each symbol is the mean ± standard error of five observations (corresponding to five plants per N-treatment, one observation per
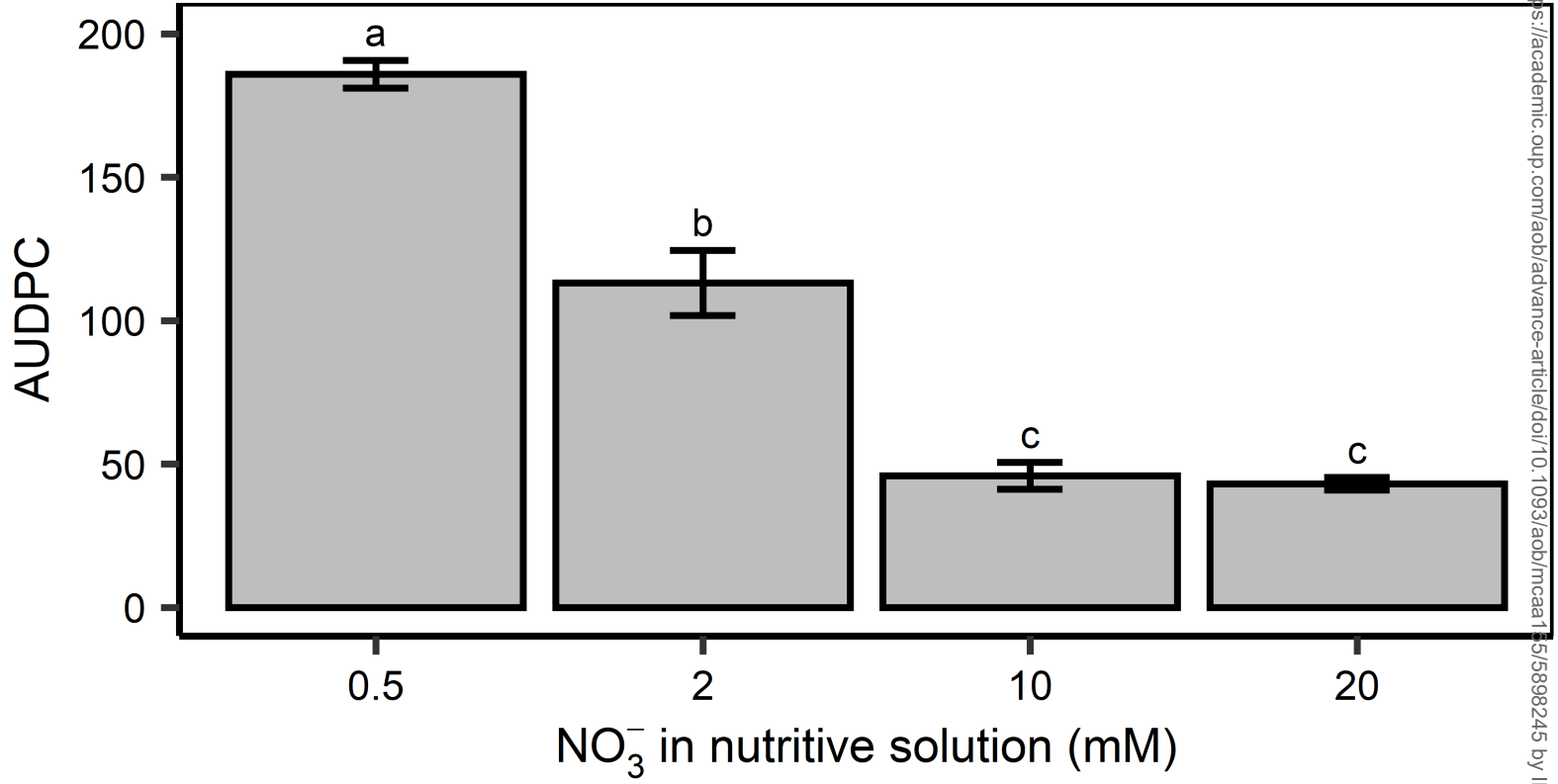
plant). Asterisks indicate the levels of the significance of difference in *Botrytis*-inoculated plants compared to mock-inoculated plants with the same combination of N-treatment × day of measurement (Kruskal-Wallis test, ** when $0.001 < P < 0.01$ and * when $0.01 < P < 0.05$).

FIG. 4: Changes in expression of genes that encode sucrose cleavage enzymes after *Botrytis* inoculation. The x-axis represents the fold change of gene expression of *Botrytis*-inoculated plants at 2, 4 or 7 days post-inoculation (DPI), compared to the gene expression of plants before inoculation. The y-axis represents the fold change of gene expression of *Botrytis*-inoculated plants compared to the gene expression of mock-inoculated plants with the same combination of N-treatment × day of measurement. The grey area represents zones under the threshold level of significance fixed at a 1.5 fold change. Genes in grey indicate no difference of expression between *Botrytis*- and mock-inoculated plants, genes in red are over-expressed and genes in blue are under-expressed.
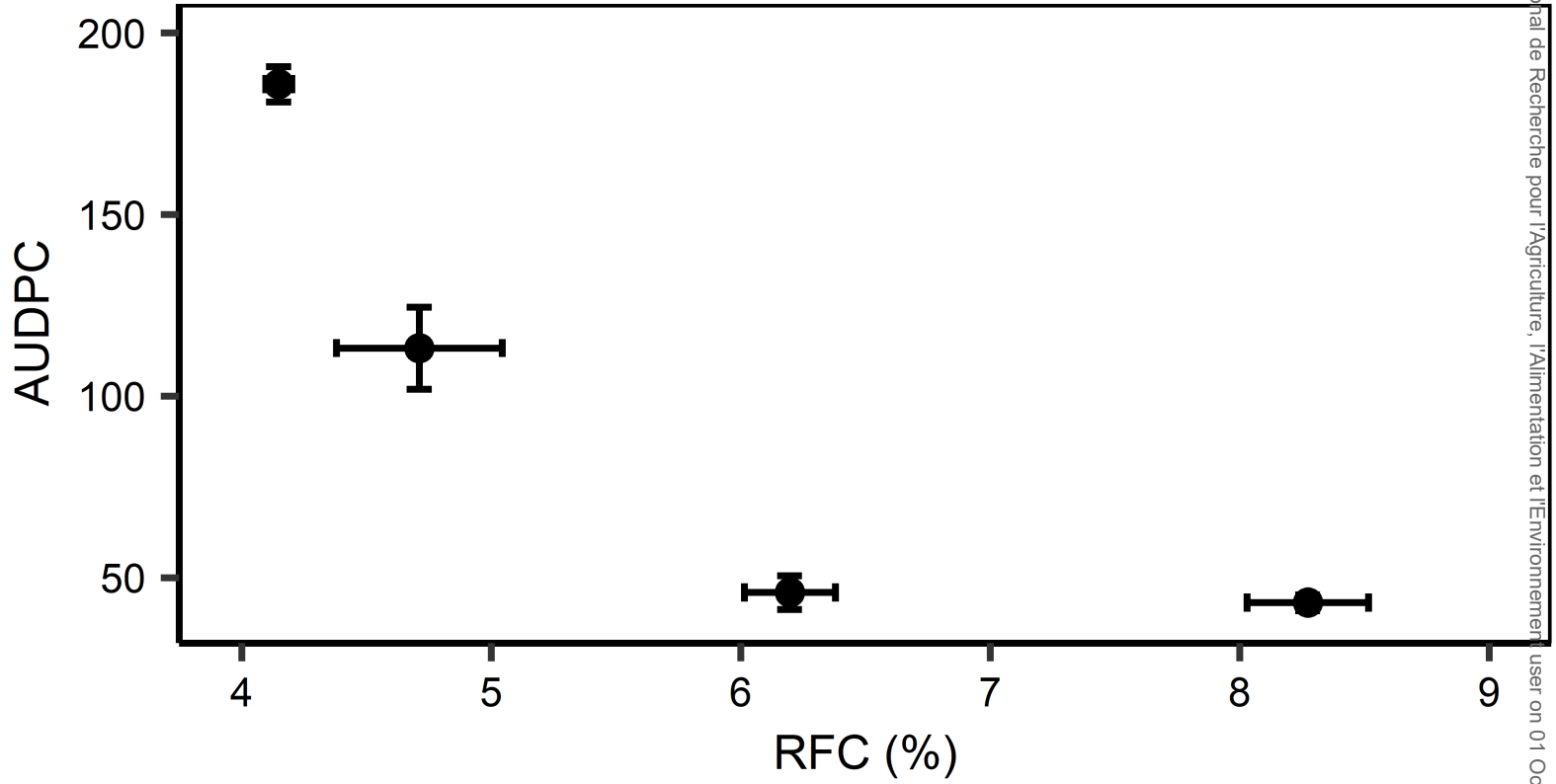
FIG. 5: Changes in expression of hexose kinase genes during *Botrytis* infection. The x-axis represents the fold change of gene expression of *Botrytis*-inoculated plants at 2, 4 or 7 days post-inoculation (DPI), compared to the gene expression of plants before inoculation. The y-axis represents the fold change of gene expression of *Botrytis*-inoculated plants compared to the gene expression of mock-inoculated plants with the same combination of N-treatment × day of measurement. The grey area represents zones under the threshold level of significance fixed at a 1.5 fold change. Genes in grey indicate no difference of expression between *Botrytis*- and mock-inoculated plants, genes in red are over-expressed and genes in blue are under-expressed.
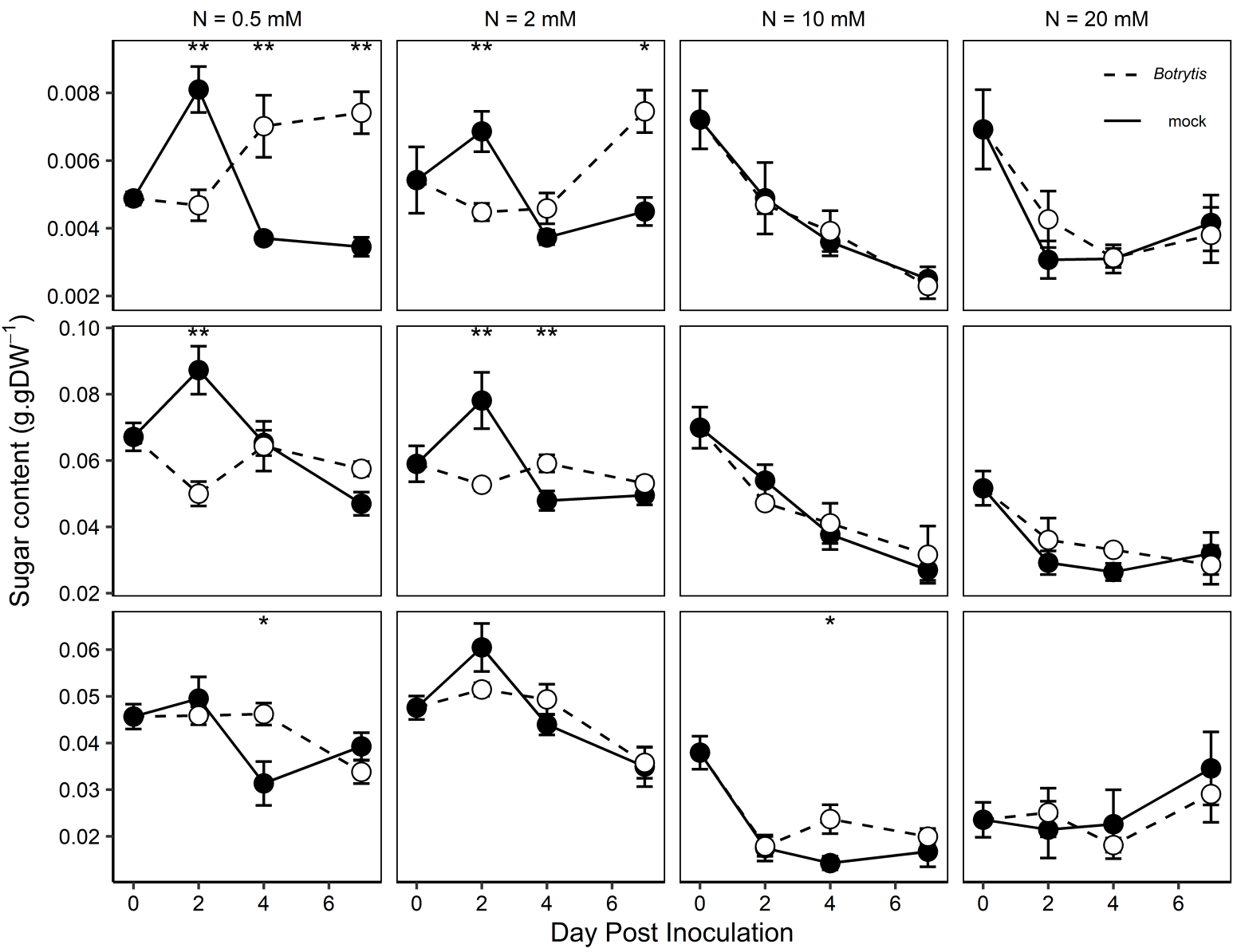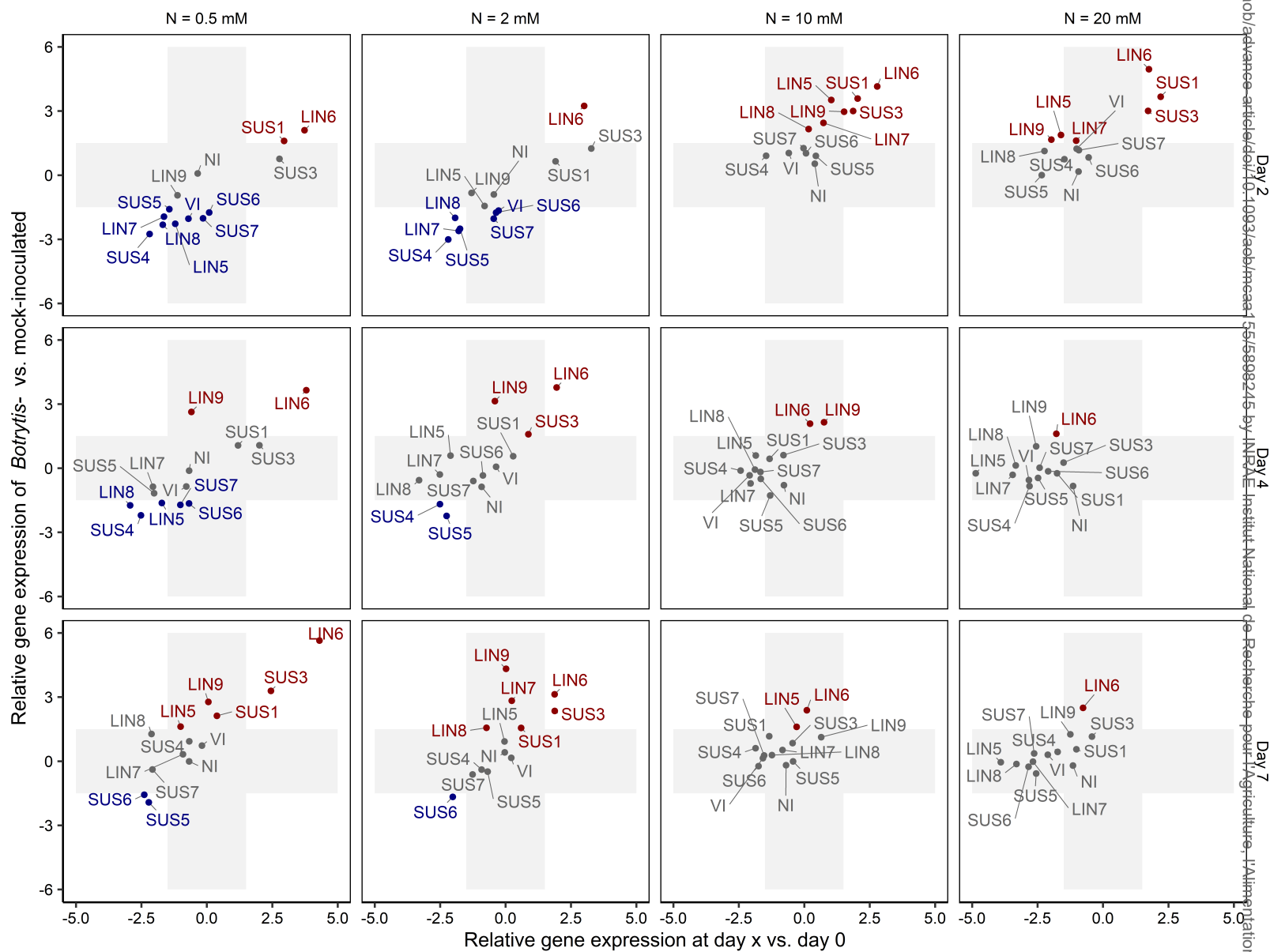
N = 0.5 mM   N = 2 mM   N = 10 mM   N = 20 mM

Fructose

Glucose

Sucrose

Sugar content (g.gDW^{-1})

Day Post Inoculation

Botrytis

mock